IX CONGRESSO BRASILEIRO DE
ENGENHARIA E CIÊNCIAS TÉRMICAS
9th BRAZILIAN CONGRESS OF THERMAL
ENGINEERING AND SCIENCES

Paper CIT02-0030

GRID ADAPTATION BASED ON A CHIMERA FRAMEWORK FOR 2D FLOW SIMULATIONS

Edson Basso
Instituto Tecnológico de Aeronáutica – CTA/ITA/IEAA
12228-900 – São José dos Campos – SP
basso@iae.cta.br

João Luiz F. Azevedo
Instituto de Aeronáutica e Espaço – CTA/IAE/ASE-N
12228-904 – São José dos Campos - SP
azevedo@iae.cta.br

Abstract. *A study of mesh refinement for overset structured multiblock grids is performed in the present work. The refinement process is based on the Adaptive Mesh Refinement (AMR) method. The increase in grid density is achieved through the application of Chimera grid techniques. The use of the Chimera grid ideas allows the creation of new mesh blocks only in the regions of interest. Regions, which require grid refinement, are identified through the definition of a sensor based on flow property gradients. For the applications of interest in the present case, flowfields are simulated using the Euler equations. The equations are discretized by a finite difference method in which spatial discretization uses 2nd-order, central difference operators, together with adequate scalar, non-linear, artificial dissipation models. Results are presented for supersonic air inlets and the numerical data is compared to analytical solutions of the problem.*

Keywords. *Adaptive mesh refinement, Chimera grids, Computational Fluid Dynamics.*

1. Introduction

The present paper is concerned with the presentation and discussion of 2-D supersonic flow simulation results, which use adaptive mesh refinement techniques in the context of Chimera grids. The work here described is a part of a larger effort aimed at developing the necessary computational tools required for the simulation of the aerodynamic flows of interest for aerospace configurations, especially those related to the VLS system (Basso et al., 2000). In particular, Basso et al. (2000) describes detailed supersonic flow simulations over the complete VLS vehicle, which is the first Brazilian satellite launcher and which has a cluster configuration with four strap-on boosters around a central core. The simulations included in the cited reference use an overset multiblock technique, or Chimera technique, in order to handle the geometric complexity of the configuration of interest. The work presented here can be seen as an extension of that shown in Basso et al. (2000) in the sense that the same Chimera framework created to treat geometric complexity is used to handle local adaptive mesh refinement for structured grids. The paper only discusses the 2-D case but, since it simply exploits the Chimera framework previously developed, the extension for the complete 3-D case should not pose any additional conceptual hurdles.

The major thrust behind the use of adaptive mesh refinement, either for structured or unstructured grids, is in the CPU time savings which may come from a judicious use of the available grid points in order to provide an adequate resolution of the relevant flow phenomena. For 2-D cases, this aspect becomes more evident when dealing with transient flows since the regions, which require additional grid refinement, may vary as the flow evolves. Hence, as the time marching progresses, the regions of interest or the more important flow phenomena are also changing with time and the grid must be able to provide the required resolution in a time-accurate manner. Another important example concerns the cases in which there is relative motion between different parts of the configuration under study. This is the case when one is concerned with store separation problems or with staging on satellite launchers. Both cases imply in relative motion of the computational domain boundaries, displacement of the relevant phenomena in the flow or, even, the arising of new flow structures, which have not been anticipated in the generation of the original mesh. For 3-D problems, the need for the use of some adaptive grid refinement strategy becomes even more emphatic, since the meshes can be very large. In this case, if the flow phenomena that requires grid refinement is quite localized, there is no justification for performing an overall refinement of the entire mesh, since this procedure could easily yield computational grids, which are beyond the available computational resources.

In this context, the present work uses an adaptive refinement technique inspired in the work of Berger (1982) and Berger and Collela (1989). This technique achieves the desired spatial resolution by the addition of new mesh blocks in the regions of interest. These regions to be refined are defined through the use of a property gradient-based sensor. The sensor is computed with a sweep over the current mesh and, clearly, using the previously calculated solution in this

mesh. This process defines regions in which the gradient of flow properties are above a certain specified threshold value. After these regions are identified, the code generates new mesh blocks, with smaller mesh spacing, in order to achieve a better spatial resolution.

Although the procedure implemented here for mesh refinement is inspired in the work of Berger and her co-workers (Berger, 1982, Berger and Collela, 1989), it is actually a fully original approach in the sense that the pre-existing flow simulation code based on the Chimera technique is fully exploited here in order to achieve the desired adaptive refinement capability. Therefore, the new grid blocks generated by the refinement procedure are added to the calculation process through the usual procedures implemented for Chimera grids. Such procedures include the logical cutting of grid points in the overset mesh regions created by the new grid blocks and the identification of block boundary points which should be treated by the usual Chimera interpolation procedure. This essentially means that block interfaces due to AMR-like adaptive refinement are treated in exactly the same fashion as block interfaces that arise on overset multiblock grids. The results presented in this paper are concerned with flow simulations in a 2-D supersonic inlet. An initial mesh is selected and, then, additional mesh blocks are added to it through the adaptive refinement procedure. Flow property values throughout the domain are compared with analytical results as part of the verification and validation process of the algorithm developed.

2. Theoretical formulation

It is assumed that the flows of interest in the present work can be represented by the Euler equations in two dimensions. These equations can be written in conservation-law form for a curvilinear coordinate system as

$$\frac{\partial \overline{Q}}{\partial \tau}+\frac{\partial \overline{E}}{\partial \xi}+\frac{\partial \overline{F}}{\partial \eta}=0\,, \tag{1}$$

where $\overline{Q}$ is the vector of conserved variables and $\overline{E}$ and $\overline{F}$ are the inviscid flux vectors, defined as

$$\overline{Q}=J^{-1}\begin{Bmatrix}\rho\\ \rho u\\ \rho v\\ e\end{Bmatrix},\quad \overline{E}=J^{-1}\begin{Bmatrix}\rho U\\ \rho uU+p\xi_x\\ \rho vU+p\xi_y\\ (e+p)U-p\xi_t\end{Bmatrix},\quad \text{and}\quad \overline{F}=J^{-1}\begin{Bmatrix}\rho V\\ \rho uV+p\eta_x\\ \rho vV+p\eta_y\\ (e+p)V-p\eta_t\end{Bmatrix}. \tag{2}$$

In these equations, ρ is the density, p is the pressure, and u and v are the Cartesian velocity components. The pressure p is obtained from the perfect gas law, written in the convenient form as

$$p=(\gamma-1)\rho e_i\,, \tag{3}$$

where γ is the ratio of specific heats and e_i is the specific internal energy. The total energy per unit volume, e, is defined as

$$e=\rho\left[e_i+\frac{1}{2}\left(u^2+v^2\right)\right]. \tag{4}$$

The contravariant velocity components, U and V, are written as

$$\begin{aligned}U&=\xi_t+\xi_x u+\xi_y v\,,\\ V&=\eta_t+\eta_x u+\eta_y v\,,\end{aligned} \tag{5}$$

and the metric terms are expressed by

$$\begin{aligned}\xi_x&=Jy_\eta, & \eta_x&=-Jy_\xi,\\ \xi_y&=-Jx_\eta, & \eta_y&=Jx_\xi,\\ \xi_t&=-x_\tau\xi_x-y_\tau\xi_y, & \eta_t&=-x_\tau\eta_x-y_\tau\eta_y.\end{aligned} \tag{6}$$

The Jacobian of the transformation, J, can be written as

$$J=\left(x_\xi y_\eta-x_\eta y_\xi\right)^{-1}. \tag{7}$$

Although in the present paper only supersonic flow is of interest, the code has a suitable change of variables, where density is replaced by pressure as a major variable of the continuity equation (Chen, 1991, Martins, 1994). The Euler equations can be rewritten as

$$\frac{\partial Q(q)}{\partial \tau} + \frac{\partial E(q)}{\partial \xi} + \frac{\partial F(q)}{\partial \eta} = 0\,, \tag{8}$$

where

$$q = \begin{Bmatrix} p \\ u \\ v \\ T \end{Bmatrix}. \tag{9}$$

The vector of conserved variables can be written as

$$Q = J^{-1}\begin{Bmatrix} \frac{p}{T} \\ \frac{pu}{T} \\ \frac{pv}{T} \\ \frac{p}{(\gamma-1)} + \frac{p}{2RT}\left(u^2+v^2\right) \end{Bmatrix}, \tag{10}$$

and the inviscid flux vectors can be rewritten as

$$E = J^{-1}\begin{Bmatrix} \frac{pU}{T} \\ \frac{puU}{T} + Rp\xi_x \\ \frac{pvU}{T} + Rp\xi_y \\ \left[\frac{\gamma p}{\gamma-1} + \frac{p}{2RT}\left(u^2+v^2\right)\right]U - p\xi_t \end{Bmatrix}, \qquad F = J^{-1}\begin{Bmatrix} \frac{pV}{T} \\ \frac{puV}{T} + Rp\eta_x \\ \frac{pvV}{T} + Rp\eta_y \\ \left[\frac{\gamma p}{\gamma-1} + \frac{p}{2RT}\left(u^2+v^2\right)\right]V - p\eta_t \end{Bmatrix} \tag{11}$$

where R is the gas constant. A suitable nondimensionalization of the governing equations has been assumed in order to write Eq. (1). In particular, in the present case, the values of flow properties are made dimensionless with respect to the entrance conditions.

The governing equations were discretized in a finite difference context on structured quadrilateral meshes, which would conform to the geometry in the computational domain. Since a central difference spatial discretization method is being used, artificial dissipation terms must be added to the formulation in order to control nonlinear instabilities. The artificial dissipation terms used here are based on a scalar, isotropic model (Pulliam, 1986). In the present implementation, the residue operator is defined as

$$RHS^n = -\Delta t\left(\delta_\xi E^n + \delta_\eta F^n\right). \tag{12}$$

Here, the δ_ξ and δ_η terms represent central difference operators in the ξ and η directions, respectively, and E and F are numerical flux vectors at the mesh mid-points. Since steady state solutions are the major interest of the present study, a variable time step convergence acceleration procedure has been implemented. In the present case, the time step is defined as

$$\Delta t_{i,j} = \frac{CFL}{c_{i,j}}\,. \tag{13}$$

The characteristic velocity $c_{i,j}$ is defined as

$$c_{i,j} = \max\left(|U| + a\sqrt{\xi_x + \xi_y}, |V| + a\sqrt{\eta_x + \eta_y}\right)_{i,j}, \tag{14}$$

where a is the speed of sound. The time march is performed based on an explicit scheme,

$$Q^{n+1} = Q^n + \Delta t\left(\frac{\partial E}{\partial \xi} + \frac{\partial F}{\partial \eta}\right)^n + \Delta t\mathcal{O}(\Delta t). \tag{15}$$

3. Boundary conditions

The physical problem treated in the present paper considers the 2-D flow in an asymmetric convergent nozzle. The nozzle entrance is assumed to be supersonic such that a shock wave is formed at the start of the convergent section of the nozzle. The attempt to adequately capture this shock wave and its reflections along the nozzle walls creates the motivation for the use of an adaptive refinement capability. The discussion in this section will, therefore, separate between the physical boundary conditions at the external boundaries of the computational domain and the internal boundaries created by the addition of grid blocks for mesh refinement.

3.1. Outer boundaries

The boundary conditions for the walls, identified in Fig. (1) by letter A, are based on the fact that there should be no flow through a solid surface. This is imposed in the present context by setting the contravariant velocity component normal to the wall to be identically zero. Aside from this boundary condition, conserved properties at the wall points are simply obtained by zero-th order extrapolation of their neighboring points in the nominally wall-normal direction.

Supersonic flow entrance conditions are imposed on the boundary identified by letter B. It should be emphasized that, since supersonic flow is being assumed at this boundary, this is a simple Dirichlet-type boundary condition in which all conserved properties are specified. Exit conditions, imposed along the C portion of the boundary, also assume supersonic flow at the exit and, therefore, they are obtained by straightforward zero-th order extrapolation of interior flow data. Clearly, the test problem was selected to simplify the boundary condition implementation and to allow the authors to concentrate on the relevant issues as far as the objectives of the paper were concerned. Hence, all test cases were selected such that one would have supersonic flow throughout the entire computational domain.

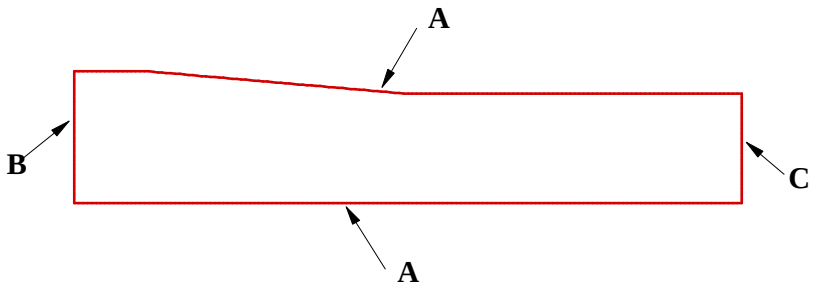

Figure 1. Domain boundaries for the initial calculation.

3.2. Inner boundaries

The internal boundaries created by the addition of new grid blocks due to the adaptive refinement process are treated through the standard interpolation procedure adopted for Chimera grids. In other words, the new grid blocks are added to the flow calculation as any other Chimera grid block. The process for adding blocks to a composite grid consists, basically, in the logical cutting of grid points in the regions of overlap, using a procedure usually called hole-cutting in the literature. A more detailed description of the hole-cutting approach used in the present case, as well as for the criteria used for point removal, can be seen in Yagua and Azevedo (1998), Yagua et al. (1999) and Basso et al. (2000). A primary reason for the decision on this form of treating the internal boundaries created by the adaptive refinement procedure was, clearly, the possibility of complete reuse of the processes already implemented in the flow simulation code under consideration. Therefore, there was absolutely no need to perform modifications in the flow solver in order to be able to handle the adapted grids. Another important reason that prompted the authors to use the current approach was the observation that there were no significant impacts in the conservative properties of the discretized equations due to the use of non-conservative interpolations, which are common practice at internal Chimera boundaries. Clearly, the use of property interpolations, which do not enforce conservation at grid block interfaces, makes the code implementation simpler and flow simulation less expensive. Hence, it is commonly accepted by the Chimera community (Benek, 1999).

One should observe that the procedure for handling the new blocks is different from that used in the original work of Berger (1982) and Berger and Collela (1989), in which the new finer grid blocks overlap the blocks already existing due to previous refinement levels but the latter are not blanked out, in a Chimera sense, as in the present paper. Therefore, in the previously cited references, no mesh point is logically cut out from the simulation and, hence, these points of previous refinement levels coexist with the new points (blocks) created by the adaptive refinement procedure.

4. Results and discussion

The results here presented are concerned with the simulation of 2-D supersonic flows in an air inlet. These results consider an inlet inflow Mach number equal to 1.6 and that the incoming flow is aligned with the inlet lower wall. All property values referred to in the paper were made dimensionless with respect to the flow properties at the inlet entrance station. All numerical solutions that are presented here have enforced more than 10 orders of magnitude drop in the L2 norm of the continuity equation residue. It is also important to emphasize that the addition of the new grid blocks due to adaptive refinement has not caused any delay in convergence when compared to solutions in a single grid. Figure (2) shows the initial mesh used in the present simulations together with 13 refined blocks generated by the process here described in a first refinement pass.

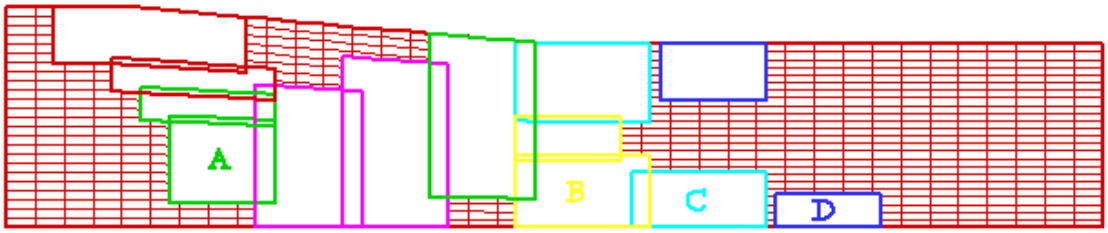

Figure 2. All refined blocks for the present calculation.

The initial mesh has a total of 39 x 25 grid points in the inlet longitudinal and crossflow directions, *i.e.*, ξ and η directions, respectively. The forthcoming discussion will present mass conservation studies across grid blocks and, for that matter, grid blocks A, B, C and D, which are used for such studies, are already identified in Fig. (2). These studies maintained the positions and dimensions of these blocks, but they have varied the number of points the blocks have in each coordinate direction. An example of such variation in the number of grid points per block is presented in Fig. (3).

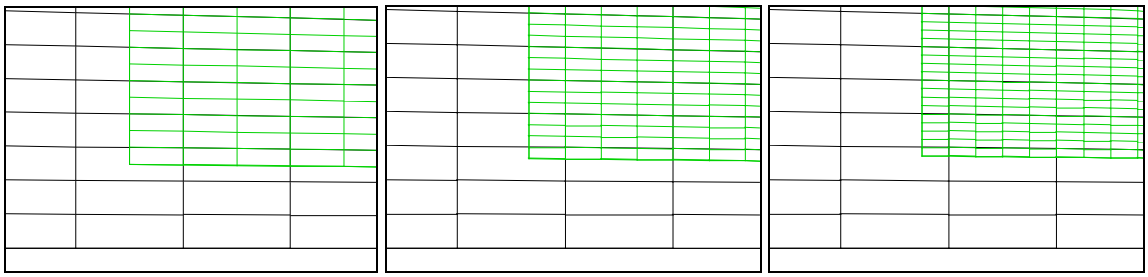

(a) (b) (c)

Figure 3. Examples of refined blocks.

For the A block, for instance, 9 x 21 points for the ξ and η directions, respectively, have been used in the simulations for the refinement denoted here as a 2X refinement. In such a case, the fine blocks had their mesh spacing reduced to half of the original spacing in the base mesh, as shown in Fig. (3a). For the case that will be labeled here 3X refinement, the A block has 12 x 30 grid points and this case is illustrated in Fig. (3b). Similarly, for the 4X refinement case, shown in Fig. (3c), the mesh has 15 x 39 grid points in the ξ and η directions, respectively.

Figure (4) presents the dimensionless pressure contours in the inlet for the 2X refinement case. One can observe in this figure that the regions with high property gradients are correctly captured through the addition of new mesh blocks added by the adaptive refinement procedure. Smooth regions of the flow and regions in which the gradients were too faint, due to the coarseness of the initial mesh, do not have any overset blocks. One can further notice in the figure that the communication of information between fine blocks, and between those and the initial mesh, was quite adequate and continuous.

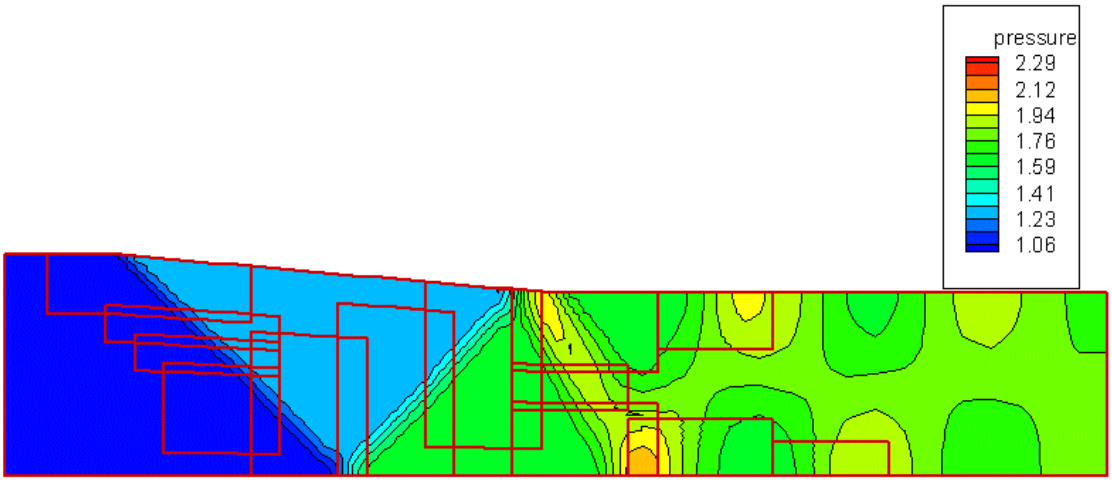

Figure 4. Pressure contour field for 2X refined blocks.

There are oscillations in the property contours only when high property gradients cross the interface between fine grid blocks and the original mesh. Numerical solutions have indicated that the oscillations are intensified when one increases the ratio of mesh spacing between adjacent blocks. This behavior was somewhat expected for two main reasons. First of all, with an increase in the number of points to be interpolated from one mesh to the other, it is reasonable to assume that the interpolation errors also increase. The other aspect is the straightforward difference in mesh cell sizes, which clearly also increases as the ratio of mesh spacing increases. The oscillations become quite evident in Fig. (5), which shows results for a 3X refinement case. The oscillations are present in the regions in which shocks or shock reflections leave the refined blocks towards the original mesh, especially in the downstream portion of the flowfield.

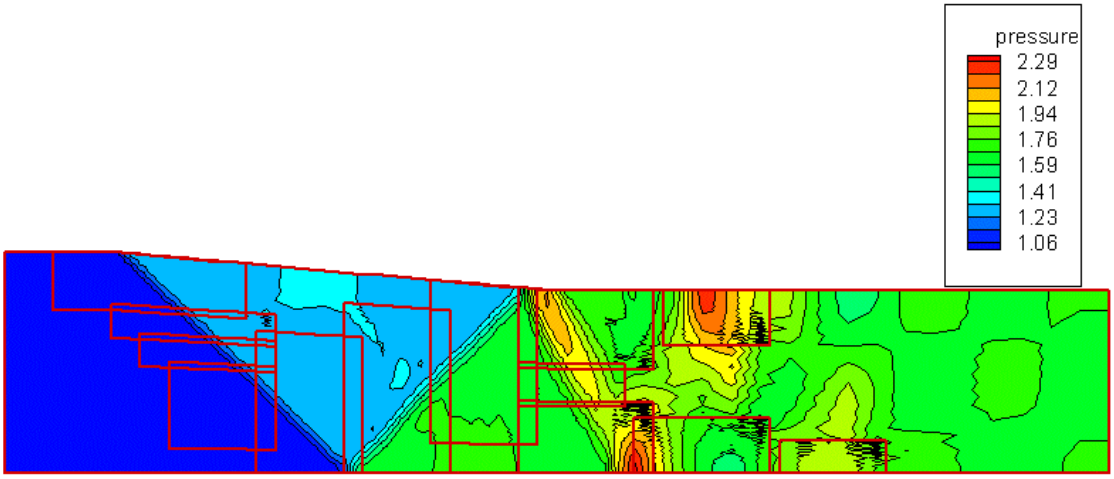

Figure 5. Pressure contour field for 3X refined blocks.

Figure (6) presents the dimensionless pressure field for blocks with a 4X-type refinement. One can observe that there are still oscillations in the same regions mentioned in the previous paragraph, but these are not as intense. At this point, the authors believe that this behavior is associated to a better resolution of the initial shock and, hence, of its reflections. Therefore, this would help provide for a better definition of the properties and of the location of the high gradient regions crossing the block interfaces.

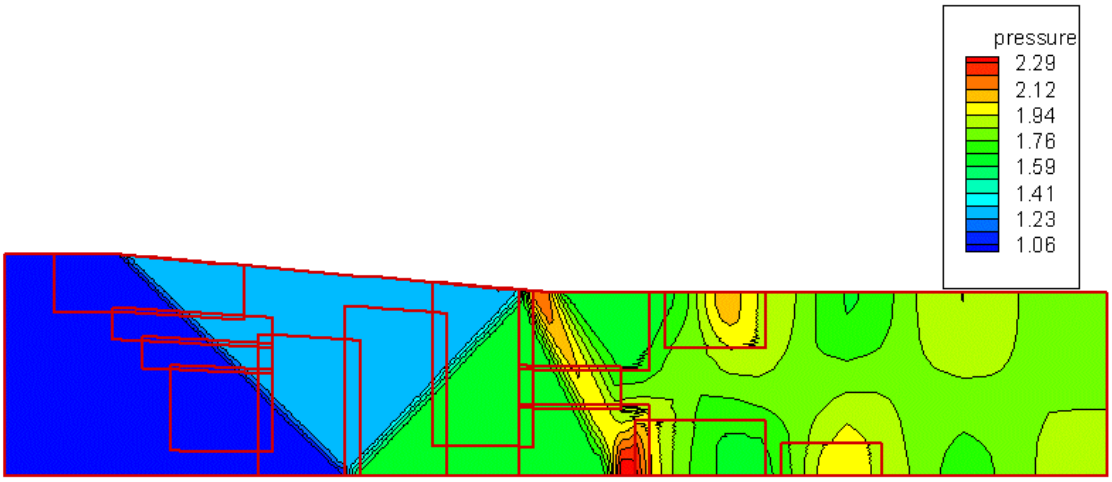

Figure 6. Pressure contour field for 4X refined blocks.

In an attempt to reduce the oscillations at those interfaces, modifications were made in the threshold values for the sensor in order to force further refinement even in regions with lower gradient values. The rationale for such an approach was to try to move the block interfaces to regions with lower property gradients. Figure (7) presents the results for one of these studies in which, after one refinement pass, one ends up with 14 fine blocks. It must be observed that the resulting refined blocks in this case are fairly different from those shown in Fig. (2), although the number of blocks is not very different. Furthermore, in this particular study, a 4X refinement was also used. The results, however, in terms of smoothness of pressure contours, as shown in Fig. (7), are not very encouraging and further work must be done in order to understand and control these block interface oscillations.

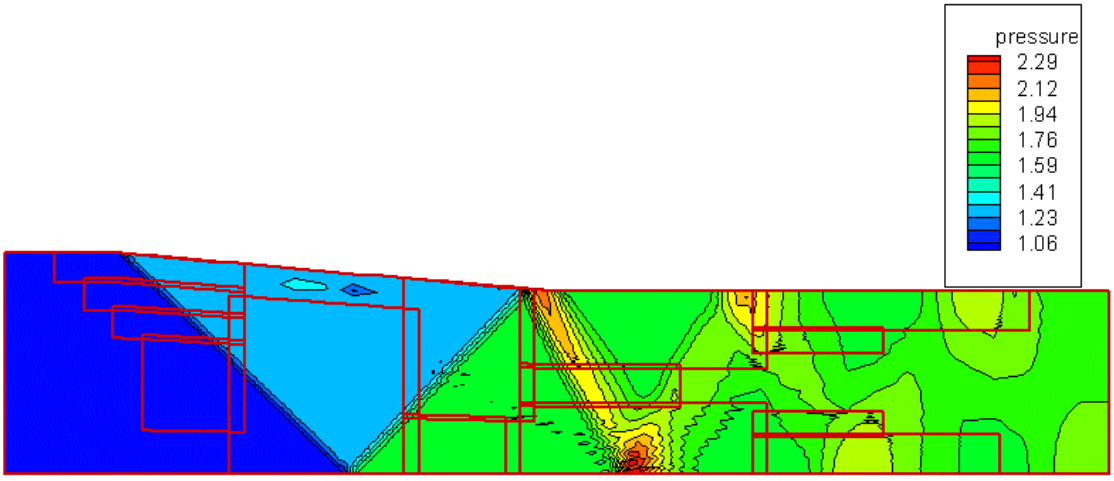

Figure 7. Pressure contour field for 4X refined blocks with 14 blocks.

The solution of the problem with a single mesh with 153 x 97 grid points in the ξ and η directions, respectively, is shown in Fig. (8) in terms of dimensionless pressure contours. The number of points in this mesh was selected such that one would obtain a mesh spacing equivalent to that achieved in the fine mesh blocks with a 4X-type refinement. Therefore, this result allows for a direct comparison with those shown in Figs. (6) and (7), since the current level of refinement for the overall mesh is identical to that obtained in the fine blocks of the former data. The comparison indicates a good qualitative agreement and the correct capture of flow topology by the adaptively refined meshes. Clearly, these have the oscillation problems, as already discussed. Nevertheless, in the refined regions, the shock resolution is essentially the same and, hence, the approach can be a good option since the adaptively refined grids result in a less expensive simulation when compared to a fully refined mesh, as the one used in the calculations of Fig. (8). As an example, for the case showed in Fig. (6), 14 blocks were used, which summed 9.497 points. This amount is about 64% of the grid presented in Fig. (8).

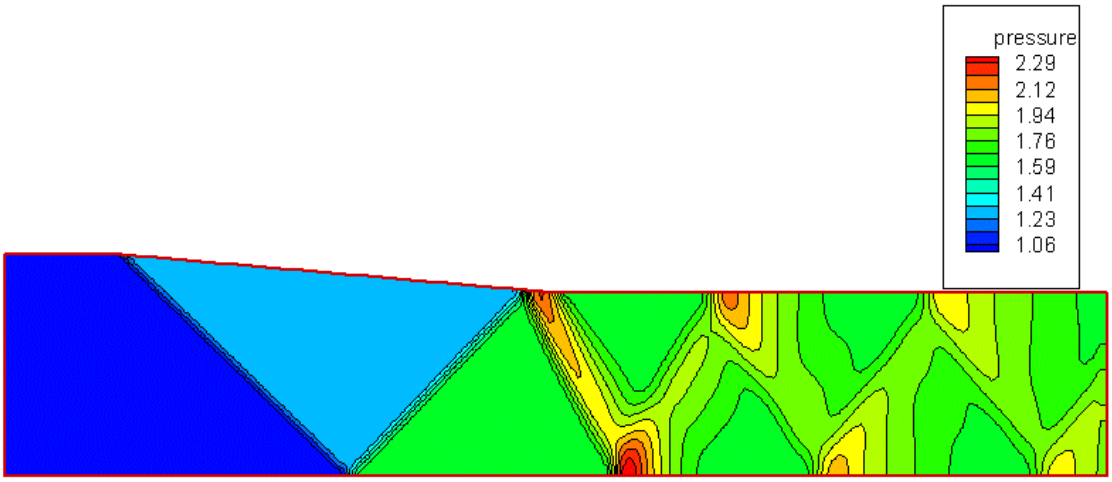

Figure 8. Pressure contour field for the base mesh.

The analytical solution of the problem or, at least, the position of the initial shock wave and its first reflection is shown in Fig. (9). The flow conditions in the three regions identified in Fig. (9) and the shock angles were calculated using the standard oblique shock relations (Anderson, 1991). This analytical solution allows for, at least, some partial quantitative comparison of the previous computational results. For region I, the Mach number is 1.6 and the dimensionless pressure is 1.0. For region II, the oblique shock relations yield that the Mach number should be 1.4368 and that the dimensionless pressure should be 1.2710. Finally, the same approach yields for region III that the Mach number is 1.2570 and the dimensionless pressure 1.6154. The calculation of the analytical solution downstream of region III becomes more complicated because the second shock reflection interacts with the expansion fan, which emanates from the expansion corner on the top wall of the inlet. A comparison of the averaged numerical property values in these three regions with the analytical solution indicates that the solution with the adaptively refined meshes is as good as the solution with the fully refined mesh. Furthermore, the differences between these numerical results and the analytical solution are within the accuracy limits of the numerical method.

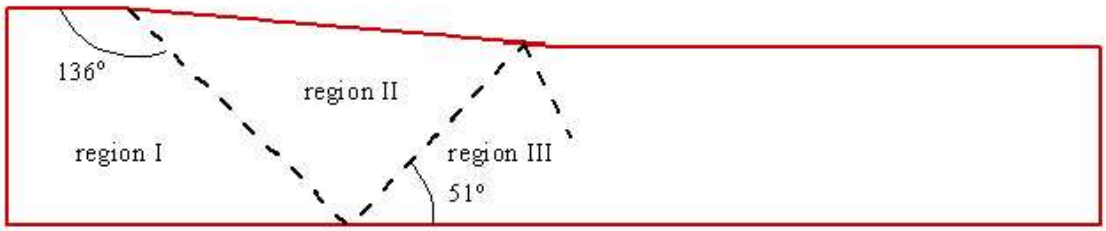

Figure 9. Representation of the analytical solution angles for the initial shock and its first reflection.

Further quantitative validation of the procedure implemented is performed through the comparisons presented in Tables (1) through (4). Table (1) presents values of the mass flow through the inlet entrance and exit boundaries for the calculation with the initial mesh, i.e., the mesh with 39 x 25 grid points. The mass flow at the entrance boundary is denoted $\dot{m}_1$ whereas the mass flow at the exit boundary is called $\dot{m}_2$. One can observe that the difference between mass flow at the entrance and exit stations is compatible with the accuracy of the numerical method used. For Tables (2), (3) and (4), the value of $\dot{m}_1$ used to compute differences is exactly the same one reported in Table (1). Table (2) presents the inlet exit mass flows ($\dot{m}_2$), and the corresponding differences $\dot{m}_1 - \dot{m}_2$, for several different simulations in which different number of fine blocks are included in the mesh. Hence, the table is showing the difference in the exit mass flow that results from the inclusion of each of the labeled refined blocks into the calculation. The blocks labeled A, B, C and D are indicated in Fig. (2) and, furthermore, the mesh used when all fine blocks are included is precisely the one shown in Fig. (2). Finally, Table (2) presents the results when a 2X refinement is performed. Tables (3) and (4) simply repeat this study for 3X and 4X refinements, respectively.

Although the results are not fully conclusive, some trends can be highlighted from the results reported in these tables. For instance, the addition of the fine blocks increases the error in the mass flow even compared to the solution in the coarse grid. There is no clear trend associated with the number of grid blocks added. For instance, in Table (2) one can see that the addition of blocks A, B and C yield a smaller error than the addition of only block A or of blocks A and

B. However, even when all fine grid blocks created based on the sensor are added, the error is again higher. It also seems clear from the results that the cases with 3X and 4X refinement yield higher error than the case with 2X refinement. It should be further emphasized that, in the present implementation, the non-conservative interpolation is only used between a fine block and the original mesh. In other words, the interpolation between fine blocks is always conservative because, in the present example, there is a complete coincidence of the boundary points of two adjacent fine blocks.

Another interesting aspect, which can be observed in Table (4), is related to the decrease in the error when all 13 fine blocks are included in the computation, as opposed to just randomly include some of these fine blocks. The result observed in this 4X refinement case is, actually, the expected behavior, although it has not been observed in the other two cases. The rationale in this case is that, by including all the blocks identified by the sensor, one would have interpolation between fine and coarse blocks only in regions of low gradients. Finally, Fig. (10) illustrates some of the results compiled in the four tables in a graphical form. This figure is showing the mass flow along several crossflow direction planes along the domain for the initial coarse mesh, as well as the exit plane mass flow for some of the cases reported in Tables (1) through (4).

Table 1. Single mesh.

mass flow ($\dot{m}_1$)	mass flow ($\dot{m}_2$)	difference $\left(\left\|\dot{m}_1 - \dot{m}_2\right\|\right)$ (%)
6.000000	5.99572945	7.11E-2

Table 2. 2X refinement.

mass flow ($\dot{m}_2$)	difference $\left(\left\|\dot{m}_1 - \dot{m}_2\right\|\right)$ (%)	refined block
5.98064870	3.22E-1	A
5.98681986	2.19E-1	A+B
6.00730714	1.21E-1	A+B+C
5.99037759	1.60E-1	A+B+C+D
6.01775318	2.95E-1	all (13 blocks)

Table 3. 3X refinement.

mass flow ($\dot{m}_2$)	difference $\left(\left\|\dot{m}_1 - \dot{m}_2\right\|\right)$ (%)	refined block
5.96970964	5.05E-1	A
5.88684844	1.88	A+B
5.87934522	2.01	A+B+C
5.87913765	2.01	A+B+C+D
5.92817206	1.19	all (13 blocks)

Table 4. 4X refinement.

mass flow ($\dot{m}_2$)	difference $\left(\left\|\dot{m}_1 - \dot{m}_2\right\|\right)$ (%)	refined block
5.98347647	2.75	A
5.98827261	1.95	A+B
6.00860789	1.43	A+B+C
5.98322801	2.79	A+B+C+D
6.04608488	7.62E-1	all (13 blocks)

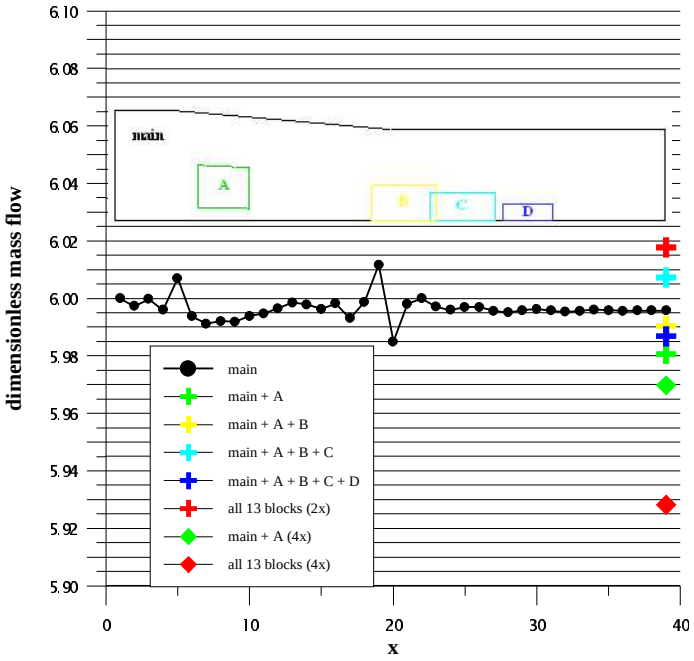

Figure 10. Mass flow calculation along the domain.

5. Concluding remarks

The present work was concerned with 2-D supersonic flow simulations in an air inlet in which local grid refinement in a structured grid context is performed through the use of a Chimera framework. The test cases analyzed had the major objective of performing an assessment of the new adaptive refinement technique implemented in the code. Clearly, the first aspect of interest was the capability of the existing Chimera framework for generating fine grid blocks that would be adequate to improve the resolution of flow features when compared to the original coarse mesh. In this context, the work attempted to evaluate the flexibility of the new approach in the generation of the fine grid blocks and the influence of the numerical parameters in the process of identifying the regions to be refined. The code that generates the fine grid blocks has exhibit good behavior with respect to the adoption of different numerical parameters for the property gradient sensor. It was possible to obtain a very good control of the fine grid block generation. Furthermore, the computational time required to generate and include these new grid blocks in the calculation process was fairly acceptable.

The paper has also evaluated qualitative and quantitative aspects of the supersonic flow solutions in the inlet. Hence, the overall flow topology as well as values of flow properties in some regions of the flowfield are compared among the numerical simulations and with the analytical solution. Shock and shock reflection angles have been compared with analytical results. An evaluation of the effect of the Chimera interpolation in the conservation properties of the calculation has also been made and the effects of gradual inclusion of fine grid blocks has been quantified. In all cases analyzed, the code behavior has been shown to be quite adequate, since the differences observed are within acceptable margins for engineering applications.

The calculations included in the paper demonstrate that the methodology proposed has a good potential for been used as an adaptive refinement procedure for the codes under development, which use the overset multiblock approach. The results have indicated that it is possible to perform local grid enrichment in a structured grid context through the use of this approach. Furthermore, although no detailed computational timing comparisons have been reported here, it is important to emphasize that the adaptively refined grids shown in the paper result in computational time savings in comparison with the corresponding fully refined meshes. It is clear, also, that the gains in computational performance in 2-D are not overwhelming. However, these gains should become increasingly more relevant as one moves to address 3-D problems and, especially, those over complex configurations. The continuation of the research here reported will extend the concepts presented in the paper to the three-dimensional case and it will apply the proposed adaptive refinement technique for flows over the VLS and other launch vehicles of interest for the Brazilian aerospace community.

6. Acknowledgments

The present work was partially supported by Conselho Nacional de Desenvolvimento Científico e Tecnológico, CNPq, under the Integrated Project Research Grant No. 522413/96-0. Additional support received from CNPq in terms of graduate scholarship for the first author is also gratefully acknowledged.

7. References

Anderson, J.D., Jr., 1991, "Fundamentals of Aerodynamics", McGraw-Hill International Editions – Aerospace Sciences Series, second edition, 772 p.

Basso, E., Antunes, A.P. and Azevedo, J.L.F., 2000, "Three Dimensional Flow Simulations over a Complete Satellite Launcher with a Cluster Configuration", AIAA Paper No. 2000-4514, Proceedings of the 18th AIAA Applied Aerodynamics Conference & Exhibit, Vol. 2, Denver, CO, pp. 805-813.

Benek, J., 1999, Private Communication, .

Berger, M.J., 1982, "Adaptive Mesh Refinement for Partial Differential Equations", Ph.D. Thesis, Stanford.

Berger, M.J. and Collela, P., 1989, "Local Adaptive Mesh Refinement for Shock Hydrodynamics", J. Computational Phys., Vol. 82, pp. 67-84.

Chen, K.H., and Pletcher, R.H., 1991, "Primitive Variable, Strongly Implicit Calculation Procedure for Viscous Flows at All Speeds," AIAA Journal, Vol. 29, No. 8, pp. 1241-1249.

Martins, R.J., 1994, "Um Método de Diferênças Finitas para Simulação de Escoamentos em Qualquer Regime de Velocidade", Master Dissertation, Instituto Tecnológico de Aeronáutica, São José dos Campos, SP.

Pulliam, T.H., 1986, "Artificial Dissipation Models for the Euler Equations," AIAA Journal, Vol. 24, No. 12, pp. 1931-1940.

Yagua, L.C.Q. and Azevedo, J.L.F., 1998, "Compressible Flow Simulation Using Overset Multiblock Grids", Proceedings of the 4th Symposium on Overset Composite Grid & Solution Technology, Aberdeen Proving Ground, Maryland.

Yagua, L.C.Q., Basso, E. and Azevedo, J.L.F., 1999, "Three Dimensional Chimera Grid Flow Simulation over Aerospace Configurations", AIAA Paper No. 99-3132, 17th AIAA Applied Aerodynamics Conference, Norfolk, VA.